International Journal of Science Engineering and Advance Technology

Resonant Current Control Of Three Phase Grid Connected Photovoltaic Inverters

V. Pranay Kumar,
M.Tech Student Scholar
EEE Dept., S.R Eng. College,
Warangal, T.S, India.

M.M. Irfan,
Asst. professor,
EEE Dept., S.R Eng. College,
Warangal, T.S, India.

Abstract: **This paper presents a new control technique used to reduce the harmonic distortion of current, without increasing the computational load of the standard current control abnormal conditions. The proposed control technique overcomes the disadvantages of resonant current control under unbalanced conditions. Simulations results of the proposed control technique are carried out and showed better performance.**

Index Terms**: Grid-Connected Photovoltaic System, Inverter.**

I. INTRODUCTION

Now a days, these PV systems are connected to the commercial utility grid [1]–[8] and also form a micro grid with other DG resources, energy storage systems, and local loads [9]–[11]. Photovoltaic (PV) power generation is an interesting concept. In recent years, a high number of PV systems with a power capacity in megawatts have appeared in the distributed generation (DG) system. Regarding with the output connection, power quality is an essential feature of PV systems. The power quality is mainly governed by practices and standards on voltage, frequency, and harmonics [12]–[14]. In assure no adverse effects are caused to other equipment connected to the utility grid or the micro grid, PV systems should have low current harmonic distortion. In practice, the maximum total harmonic distortion (THD) of 5% is accepted at rated inverter output [12]. The resonant current control has been used to reduce the current harmonic distortion in a DG applications [15]–[21], including PV systems [22]–[24], wind and water turbines [23]–[26], and fuel-cell inverters [27], [28].

This control uses a proportional-resonant (PRES) compensator to track the fundamental component of the current reference signal and a resonant harmonic (RESH) compensator to attenuate the most important current harmonics [18], [23]. Since the resonant compensators are capable of tracking sinusoidal references of arbitrary frequency with zero steady state error [17] the satisfactory results are easily achieved with this control. The performance deterioration given by abnormal conditions is the main problem of the resonant current control in the uti132lity grid and in this condition, the grid voltage harmonics and phase imbalances may create current reference signals with non sinusoidal distorted waveforms. Also, grid voltage inter-harmonics which often appear in standard variable speed drive applications which produce distorted reference signals. As a result, the current harmonic distortion is increased due to the ability of the resonant current control to track the distorted reference waveforms accurately. Several advanced control schemes, which are characterized by a high harmonic rejection capability, have been recently introduced to cope with the formulated problem [29]–[34]. In these control schemes, the current references are generated by separately processing the positive and negative sequence components. To generate good-quality sequence components which not affected by voltage harmonics, inter-harmonics, and imbalances, the phase-locked loop (PLL) algorithms are also required [33], [34].

An increase in both the control and computational load due to the drawbacks of these control solutions. As an interesting alternative, high harmonic rejection capability is achieved for single-phase applications in [35] and [36]. In these works, instead of the typical parallel configuration of the standard resonant current control, the RESH compensator is connected in series with the PRES compensator [23], [24]. Similar to the standard one, even during polluted grid conditions low current distortion is obtained with a simple control structure. As a starting point, in this paper, the main idea introduced in [35] and [36], that is, it is possible to

inject a grid current with low distortion simple resonant control scheme.

A simple control scheme is a good alternative of previous control solutions for voltage source three-phase PV inverters which connected to the utility grid. In this control, PRES and RESH compensators are connected in parallel as opposed to the controllers in [35] and [36]. This control configuration is different from the standard resonant control [24].The resonant control improves the current harmonic distortion even in the case that the current references exhibit distorted waveforms. Thus, the high harmonic rejection capability and low computational load as compared with the standard resonant current control are the main contribution of the resonant current control intended for three-phase applications.

II. THREE-PHASE GRID-CONNECTED PV INVERTER

Three-phase PV inverter includes a PV array, a dc-link capacitor, and a three-phase voltage-source inverter shown in fig.1.and the switches of the inverter are governed by the discrete variables u, which can take the value −1 or 1. To reduce the high frequency switching harmonics the inverter employs an LCL filter with small resistive parasitic elements are considered. Also, a damping resistor is connected in series with the capacitors in order to attenuate the LCL peak magnitude at the resonance frequency and the losses in this resistor are negligible. The utility grid is modeled as three ac voltage sources.

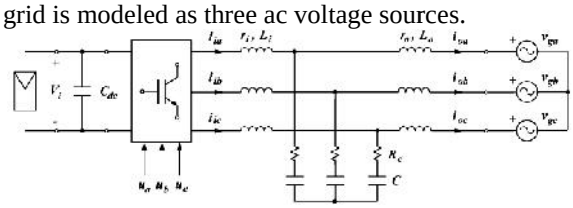

Fig.1. Three phase PV inverter

A. Open-loop Model of the Three-Phase PV Inverter

For the analysis of the resonant current control is an averaged model of the three-phase PV inverter is required and the averaged model in the stationary reference frame is shown in Fig. 2. The inputs of the model are the dc-link voltage V_i, the grid voltage vg, and the control inputs d, which can take continuous values inside the range

$$-1 \le d_\alpha \le 1 \qquad (1)$$

$$-1 \le d_\beta \le 1 \qquad (2)$$

The outputs of the model are the inverter current i_i and the grid current i_0.

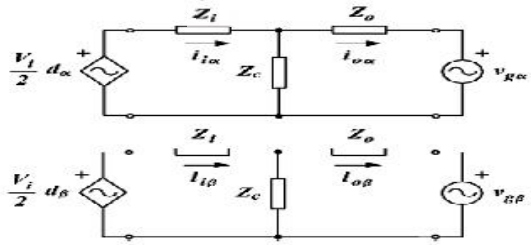

Fig.2 Averaged model of the Three-phase PV inverter.

B. Resonant Current Control

The standard configuration of resonant current control is shown in Fig.3. The error between the inverter current and the reference signal is processed by PRES compensator H1(s) and the RESH compensator H2(s) which is connected in parallel. Instead of the grid current, the inverter current is normally employed in the control which reduces the number of the required current sensors and increases the system robustness. As feed forward signals the grid voltage and the dc-link voltage are used to improve the dynamics of the system and to reject external disturbances.

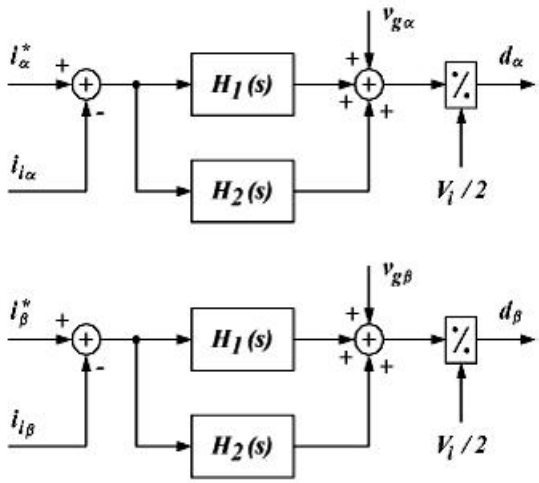

Fig.3 Standard configuration of the resonant current control

From Fig. 3, the control inputs can be written as

$$d_\alpha = \frac{2}{Vi}\,[V_{g\alpha} + (H_1(s) + H_2(s))\,(i_\alpha^* - i_\alpha)]H_{d(s)} \qquad (3)$$

$$d_\beta = \frac{2}{Vi}\,[V_{g\beta} + (H_1(s) + H_2(s))\,(i_\beta^* - i_\beta)]H_{d(s)} \qquad (4)$$

$H_d(s)$, not shown in Fig. 3, is the transfer function that models the control processing time delay Td

$$H_{d(s)} = e^{-Tds}. \quad (5)$$

C. Closed-Loop Model of the Three-Phase PV Inverter

The analysis of closed-loop dynamic model is derived by placing (3) and (4) into the open-loop model shown in Fig. 2, resulting in

$$i_{0\alpha(s)} = G_r(s) i_\alpha^*(s) + G_g(s) V_{g\alpha}(s) \quad (6)$$

$$i_{0\beta(s)} = G_r(s) i_\beta^*(s) + G_g(s) V_{g\beta}(s) \quad (7)$$

Where the reference-signal-to-grid-current transfer function and the grid-voltage-to-grid-current transfer function can be expressed, respectively, as

$$G_r(s) = \frac{Zc(s)Gi(s)\,(H1(s) + H2(s))Hd(s)}{1 + T(s)} \quad (8)$$

$$G_g(s) = -\frac{Gi(s)\,(Zi(s) + (H1(s) + H2(s))Hd(s)}{1 + T(s)} \quad (9)$$

Moreover, the loop gain T(s) and the transfer function $G_i(s)$ can be written as

$$T(s) = (Z_c(s) + Z_0(s))G_i(s) \times (H_1(s) + H_2(s))H_d(s) \quad (10)$$

$$G_i(s) = \frac{1}{Zi(s)\,(Zc(s) + Zo(s)) + Zc(s)Zo(s)} \quad (11)$$

It is mentioned that the closed-loop dynamics of the grid current does not depend on the dc-link voltage shown in (6) and (7) and this fact can be attributed to the feed forward action which introduced in (3) and (4) by the dc-link voltage signal. Grid voltage of feed forward signal is also included in the control inputs (3) and (4). In this case, the closed-loop dynamics of the grid current is affected by grid voltage disturbances through the transfer function $G_g(s)$ and this transfer function presents significant magnitude attenuation in the frequency range. Therefore, the direct influence of the grid voltage disturbances on the grid current is nearly negligible.

III. ANALYSIS AND LIMITATIONS OF THE STANDARD RESONANT CURRENT CONTROL

The standard resonant current control employs two resonant PRES compensator H1(s) and the RESH compensator H2(s) which connected in parallel, as shown in Fig.3. The PRES compensator track the fundamental component of the current reference signal and the RESH compensator attenuates the grid current harmonics. Both compensators can be written as:

$$H_1(s) = K_p + \frac{K_{i1} 2\xi_1 \omega_0 s}{s^2 + 2\xi_1 \omega_0 s + \omega_0^2} \quad (12)$$

$$H_2(s) = \sum_n \frac{K_{in} 2\xi_n (n\omega_0) s}{s^2 + 2\xi_n (n\omega_0) s + (n\omega_0)^2} \quad (13)$$

Table I shows the three-phase system parameters value of these compensators. The standard resonant current control emerge features from the transfer functions (8)–(10). The Bode diagrams of these functions are shown in Fig. 4. Note that Fig. 4(a) shows the system is stable with a phase margin of 38.4◦ at the crossover frequency of 1.1 kHz and Fig. 4(b) shows the grid voltage- to-grid-current transfer function $G_g(s)$ has significant magnitude attenuation in the frequency range of interest (i.e., $G_g(s) \rightarrow 0$ in this frequency range). Thus, from (6), it is observed that the grid voltage disturbances do not affect the grid current dynamics and the reference-signal-to-grid-current transfer function $G_r(s)$ has a flat 0-dB magnitude within the system bandwidth shown Fig. 4(c). This ensures that even in the undesired situation the grid current tracks the reference signal accurately which has significant harmonics. Consequently, from (6), the harmonic distortion present in the reference signal may be caused by grid disturbances such as voltage harmonics or imbalances will be transferred to the grid current. This is, in fact, using the standard resonant current control which is an indirect mechanism to increase the output current harmonic distortion through grid voltage disturbances.

IV. RESONANT CURRENT CONTROL OF THREE PHASE GRID-CONNECTED PHOTO VOLTAIC INVERTERS.

The main objective of the proposed control is to achieve low harmonic distortion in the grid current even during grid abnormal conditions. This feature should be accomplished without increasing the control computational load.

A. Control scheme

Fig. 5 shows the diagram of the resonant current control of three phase grid-connected photo voltaic inverters scheme and this scheme is very similar to the standard control shown in Fig. 3. As feed forward signals, the grid voltage and the dc link voltage are included. This control scheme also has two resonant compensators, but in that case, inverter current is the input of the compensator located on the bottom instead of the error between this current and the

reference signal. This is one of the differences between the standard and this control schemes. The control objectives are reached if the resonant compensators are chosen as follows:

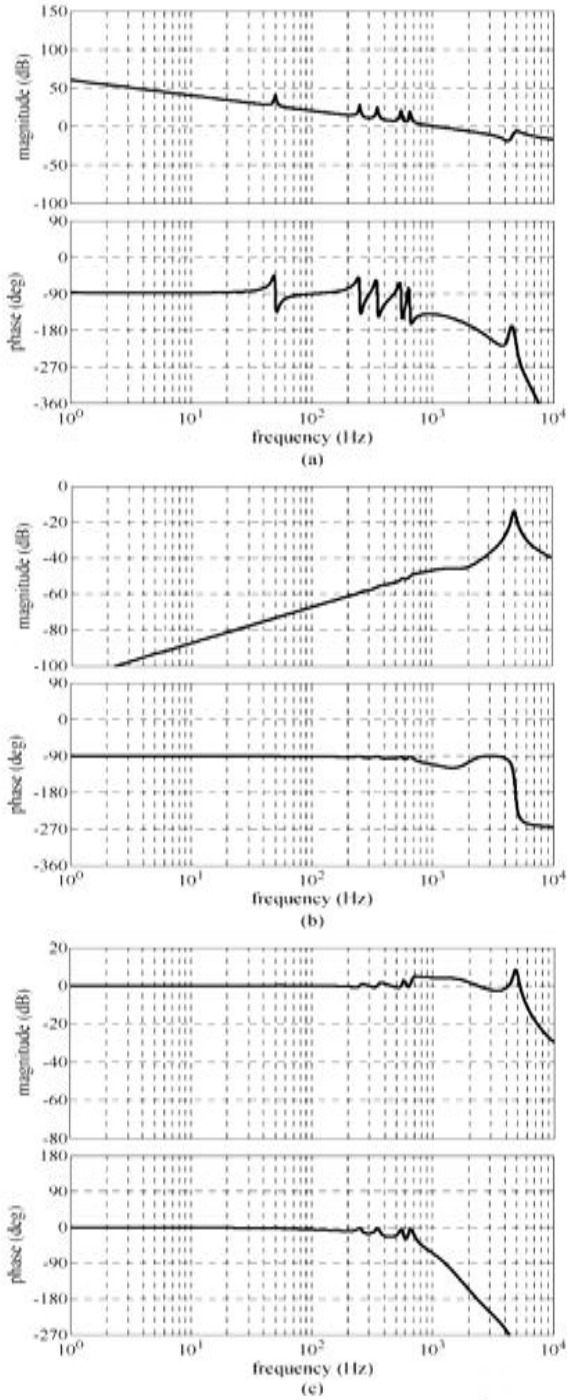

Fig.4. Bode diagrams of the standard resonant current control. (a) Loop gain transfer function T(s) (b) grid-voltage to grid- current transfer function $G_g(s)$ (c) reference signal to grid current transfer function $G_r(s)$.

$$H_3(s) = \frac{K_{i1}2\xi_1\omega_0 s}{s^2 + 2\xi_1\omega_0 s + \omega_0^2} \quad (14)$$

$$H_4(s) = K_p + \sum_n \frac{K_{in}2\xi_n(n\omega_0)s}{s^2 + 2\xi_n(n\omega_0)s + (n\omega_0)^2} \quad (15)$$

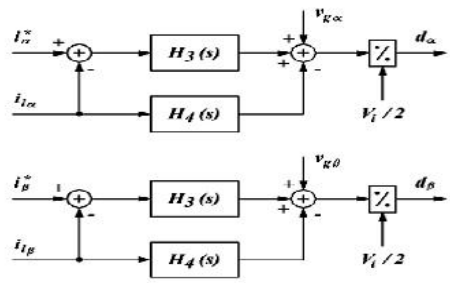

Fig.5 Resonant current control

Note that the first compensator includes only with the fundamental resonant term and the second compensator compresses both the proportional and the harmonic resonant terms and it is mentioned that

$$H_1(s) + H_2(s) = H_3(s) + H_4(s) \quad (16)$$

So that it is expected to achieve the same computational load with both control schemes.

B. Closed-Loop Transfer Functions

From Fig. 5, the control inputs of this scheme can be written as

$$d_\alpha = \frac{2}{Vi}\,[V_{g\alpha} + (H_3(s)(i_\alpha^* - i_\alpha) + H_4(s)i_{i\alpha}]H_{d(s)} \quad (17)$$

$$d_\beta = \frac{2}{Vi}\,[V_{g\beta} + (H_3(s)(i_\beta^* - i_\beta) + H_4(s)i_{i\beta}]H_{d(s)} \quad (18)$$

The closed-loop transfer functions of this control scheme are derived by inserting (17) and (18) in the open-loop model shown in Fig. 2, resulting in

$$T(s) = Z_c(s) + Z_0(s))G_i(s)(H_3(s) + H_4(s)) \times H_d(s) \quad (19)$$

$$G_r(s) = \frac{Zc(s)Gi(s)H3(s)Hd(s)}{1+T(s)} \quad (20)$$

$$G_g(s) = -\frac{Gi(s)\,(Zi(s) + (H3(s) + H4(s))Hd(s))}{1 + T(s)} \quad (21)$$

It is mentioned that the transfer functions do not depend on the steady-state values of d and Vi. This fact can be attributed to the use of the feed forward signal Vi in the control input generation shown in (3) and (4).

Taking into account (16), it is easy to prove that the loop gain and the grid-voltage-to-grid-current transfer

functions coincide with (9) and (10). As a consequence, the measures obtained from Fig. 4(a) and (b), including the relative stability, crossover frequency, and direct rejection capability of grid voltage disturbances, are also valid for this control scheme. The reference-signal-to-grid-current transfer function is, however, quite different from that shown in Fig. 4(c). Instead of a flat shape this transfer function has a band-pass filter behavior shown in Fig. 8. Note that 0-dB gain is only achieved at the grid frequency. In addition, high dips in the magnitude diagram are noticed at the selected harmonic frequencies (250, 350, 550, and 650 Hz). It is interesting to note that inter-harmonics with frequencies not located in the vicinity of integer harmonics will experience a high attenuation. This is a feature of this control scheme which is not shared by the standard control scheme shown in Fig. 4(c). As a consequence, an accurate tracking of the fundamental component of the current reference signal is expected in this control scheme and also, the reference signal integer harmonics and inter-harmonics are strongly attenuated, and therefore, a low harmonic distortion of the grid current is also expected in this control scheme.

V. SIMULINK MODEL AND RESULTS

This section verifies the resonant current control of three phase grid-connected photo voltaic inverters. A performance comparison with the standard and some selected advanced controls is also reported.

A. Simulation Model

Fig.6 shows the simulation model of the three-phase grid-connected PV inverter system consists of a dc source, three-phase inverter, and an ac programmable source. The simulation model is completed with a 4-kW resistive load connected in parallel with the ac source. This local load is necessary in the model since the ac source cannot absorb the active power which is injected by the inverter.

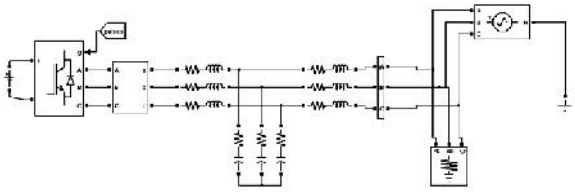

Fig.6. simulation model of the three phase grid connected PV inverter.

The digital control platform employed in the simulation model is based on a floating-point. Fig.7shows a diagram of the complete control system, it includes the conventional external control loops, i.e., the dc-link voltage regulation loop, the reactive power regulation loop, and the PLL. The diagram of the internal control loops and the space vector modulator is shown in Fig. 7(b) and the values of the control loop parameters are listed in Tables 1 and 2.

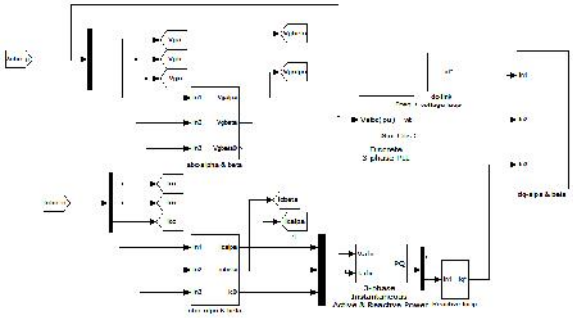

Fig.7.(a) External control system.

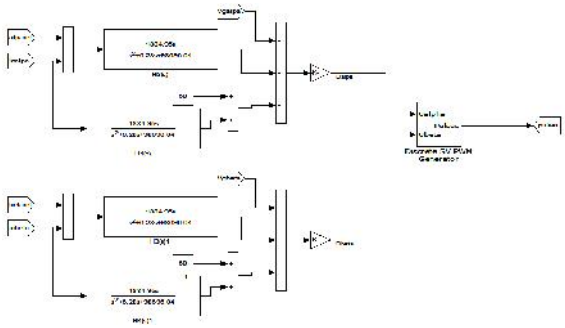

Fig.7.(b) Internal control system of modulator.

B. Current THD Measures

An extensive set of measures has been carried out in order to compare the current harmonic distortion provided by the standard and this resonant control schemes. The first set of simulation considers an ideal grid situation, i.e., the voltage supplied by the ac source has both negligible harmonics and no appreciable imbalance. The second set of simulation considers a grid with high voltage distortion. The simulation waveforms for this case are shown in Fig.8 and different voltage harmonic contents were programmed in the ac source for each grid phase. Note that when the RESH compensator is not connected, the performance of the standard current control is poor. In particular, phase c current has a harmonic distortion that exceeds the THD limits. By connecting the RESH compensator improves the performance of the standard current control. In fact, the current THD is reduced in this case, and all measures are well below the 5% limit.

Grid Current THD for a grid condition with high voltage THD and voltage imbalance

Control scheme	[illegible]	[illegible]	[illegible]	[illegible]	[illegible]	[illegible]
Standard w/o RESH	5.3	5.5	7.2	6.9	6.0	6.6
Standard with RSH	5.2	5.5	7.4	6.2	5.3	5.1
Proposed control	5.3	5.6	7.4	1.0	1.0	1.3

This control scheme further reduces the harmonic distortion and leads the current THD to almost negligible levels. The last set of simulation considers a grid with voltage harmonics and imbalances. The grid voltage magnitudes are expressed in per unit and phases are expressed in degrees. Fig.8 shows the simulation measures. Note that due to the reduction of the grid voltage the current is increase. Basically, the dc-link voltage control loop has enlarged the amplitude of the current reference signals maintain constant active power.

Simulation results

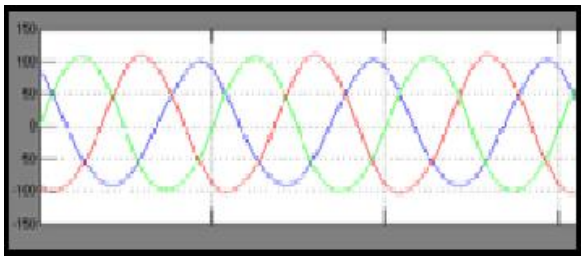

(a)

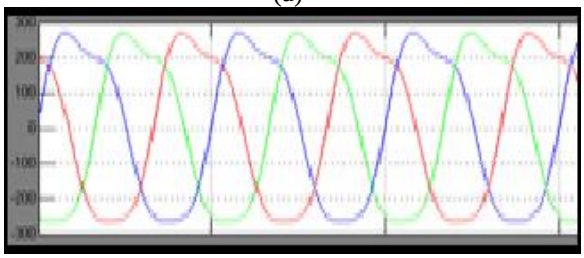

(b)

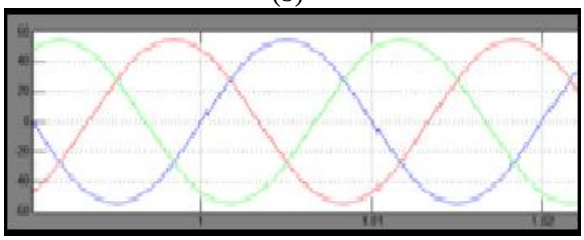

(c)

Fig.8. shows the simulation results of resonant current control of three phase grid connected PV inverters. (a) Controller current of the proposed system (b) Grid voltage of the proposed system. (c) Load current of the proposed system.

Even the RESH compensator is used in the standard control, the current THD of the three phases exceeds the limit. But in this resonant current control scheme, the current THD is low and similar to the value measured when the grid has no voltage imbalance. This feature should be attributed to the ability of this control to eliminate the harmonics present in the current reference signals. It is mentioned that the injected currents exhibit a small amplitude mismatch produced by the voltage imbalance. It is expected that this small mismatch has insignificant adverse effects on the power system.

TABLE 1
PARAMETERS OF EXTERNAL CONTROL LOOPS

Symbol	Quantity	Nominal value
[illegible]	Sampling frequency	10kHz
[illegible]	Proportional gain of SRF PLL	1.77rad/(Vs)
[illegible]	Integral gain of SRF PLL	157.91rad/([illegible])
Q*	Reference signal of the reactive power control loop(Q Loop)	0Var
[illegible]	Proportional gain of Q loop	0.001([illegible])
[illegible]	Integral gain of Q loop	0.001([illegible])
[illegible]	Reference signal of the dc-link voltage control loop (DC loop)	650v
[illegible]	Proportional gain of the DC-link loop	0.005A/V
[illegible]	Integral gain of the DC-link loop	0.01A/([illegible])

TABLE 2
PARAMETERS OF THE THREE-PHASE GRID CONNECTED SYSTEM

Symbols	Quantity	Nominal value
[illegible]	Maximum output power	3.2kw
[illegible]	Switching frequency	10khz
[illegible]	Open-circuit PV array output voltage	750v
[illegible]	Short- circuit PV array output voltage	5.4A
[illegible]	Inverter side inductance	6.9mH
[illegible]	Inverter side parasitic resistance	0.27Ω
C	Filter capacitors	680nF
[illegible]	Filter damping resistance	6.8Ω
[illegible]	Grid side inductance	2.1mH
[illegible]	Grid side parasitic resistance	0.14Ω
[illegible]	Grid voltage(rms, phase to neutral)	200v
[illegible]	Grid frequency	50Hz
[illegible]	Proportional gain	60 Ω

K_{i1}	Fundamental integral gain	300Ω
K_{in}	n-harmonic integral gain	300Ω
ξ_1	Fundamental damping factor	0.01
ξ_n	n-harmonic damping factor	0.01
N	Selected harmonics to be attenuated	5,7,11,13
T_d	Control processing delay time	100µs

C. Computational Load Measures:

The execution time of the standard and this resonant current control schemes has been measured and this control scheme has the same computational load as the standard control with RESH compensators but with a higher current harmonic rejection capability. In this study, the PLL algorithm is employed to measure the execution time of these control schemes and formulated in the stationary reference frame. Based on the ideas introduced, this control also uses symmetrical sequence components for the current reference generation. For practical application, this control scheme requires a sophisticated frequency-locked loop (FLL) for grid synchronization. The FLL is used in this project to measure the execution time of this control approach.

VI. CONCLUSION

The proposed resonant current control of three-phase PV inverters connected to the utility grid in order to attenuate the current harmonics. This controller breaks the disturbance injection mechanism by employing the same compensators that the standard current control uses but inter-connected in a different configuration. The main feature of this controller is to low the current harmonic distortion and low computational load. Simulation of the proposed system is done by using Simulink/Mat-lab. The simulation model is presented in the paper and the results are found to be better.

REFERENCES

1. E. Figueres, G. Garcerá, J. Sandia, F. González-Espin,and J. C. Rubio,"Sensitivity study of the dynamics of three-phase photovoltaic inverters with an LCL grid filter," *IEEE Trans. Ind. Electron.*, vol. 56, no. 3,pp. 706–717, Mar. 2009.
2. M. Cacciato, A. Consoli, R. Attanasio, and F. Gennaro, "Soft-switchingconverter with HF transformer for grid-connected photovoltaic systems,"*IEEE Trans. Ind. Electron.*, vol. 57, no. 5, pp. 1678–1686, May 2010.
3. R. Kadri, J. P. Gaubert, and G. Champenois, "An improved maximum power point tracking for photovoltaic grid-connected inverter based-on voltage oriented control," *IEEE Trans. Ind. Electron.*, vol. 58, no. 1,pp. 66–75, Jan. 2011.
4. N. A. Rahim, K. Chaniago, and J. Selvaraj, "Single-phase sevenlevel grid-connected inverter for photovoltaic system," *IEEE Trans. Ind. Electron.*, vol. 58, no. 6, pp. 2435–2443, Jun. 2011.
5. C. Yuen, A. Oudalov, and A. Timbus, "The provision of frequency control reserves from multiple microgrids," *IEEE Trans. Ind. Electron.*, vol. 58, no. 1, pp. 173–183, Jan. 2011.
6. D. N. Zmood, D. G. Holmes, and G. H. Bode, "Frequency-domain analysis of three-phase linear current regulators," *IEEE Trans. Ind. Appl.*, vol. 37, no. 2, pp. 601–610, Mar./Apr. 2001.
7. D. N. Zmood and D. G. Holmes, "Stationary frame current regulation of PWM inverters with zero steady-state error," *IEEE Trans. Power Electron.*,vol. 18, no. 3, pp. 814–822, May 2003.
8. T. L. Lee and S. H. Hu, "Resonant current compensator with enhancementof harmonic impedance for LCL-filter based active rectifiers," in *Proc.IEEE APEC*, 2011, pp. 1538–1543.
9. M. Liserre, R. Teodorescu, and F. Blaabjerg, "Stability of photovoltaic and wind turbine grid-connected inverters for a large set of grid impedance values," *IEEE Trans. Power Electron.*, vol. 21, no. 1, pp. 263–272,Jan. 2006.
10. J. Hu, Y. He, L. Xu, and B.Williams, "Improved control of DFIG systems during network unbalance using PI-R current regulators," *IEEE Trans.Ind. Electron.*, vol. 56, no. 2, pp. 439–451, Feb. 2009.
11. M. Andreica Vallet, S. Bacha, I. Munteanu, I. Bratcu, and D. Roye, "Management and control of operating regimes of cross-flow water turbines,"*IEEE Trans. Ind. Electron.*, vol. 58, no. 5, pp. 1866–1876, May 2011.
12. S. Y. Park, C. L. Chen, J. S. Lai, and S. R. Moon, "Admittance compensation in current loop control for a grid-tie LCL fuel cell inverter," *IEEE Trans. Power Electron.*, vol. 23, no. 4, pp. 1716–1723, Jul. 2008.
13. P. Rodríguez, J. Pou, J. Bergas, J. I. Candela, R. P. Burgos, and D. Boroyevich, "Decoupled double synchronous reference frame PLL forpower converters control," *IEEE Trans. Power Electron.*, vol. 22, no. 2,pp. 584–592, Mar. 2007.

14. F. Wang, J. L. Duarte, and M. A. Hendrix, "Pliant active and reactivepower control for grid-interactive converters under unbalanced voltagedips," *IEEE Trans. Power Electron.*, vol. 26, no. 5, pp. 1511–1521,May 2011.
15. M. Castilla, J. Miret, J. Matas, L. Garcia de Vicuna, and J. M. Guerrero,"Linear current control scheme with series resonant harmonic compensatorfor single-phase grid-connected photovoltaic inverters," *IEEE Trans.Ind. Electron.*, vol. 55, no. 7, pp. 2724–2733, Jul. 2008.

VIJAYAGIRI PRANAY KUMAR currently pursuing his M.Tech in Power Electronics from S.R Engineering College (Autonomous), Warangal, Telangana, India, affiliated to JNTU University, Hyderabad. He has done his B.Tech degree from Kamala institute of technology & science, affiliated to JNT University, Hyderabad, Telangana, India and his fields of interest include Power Systems.

M.M. IRFAN is received the B.tech degree Electrical and Electronics Engineering from ADAMS engineering college, Paloncha, Khammam, affiliated to JNTU University, the M.tech degree in Power Electronics from S.R Engineering College, Telangana state and he is currently working as Assistant Professor of EEE department at S.R Engineering College (Autonomous), Under JNTUH university of Hyderabad, Warangal(dist), Telangana, India.